

# The p75 receptor mediates axon growth inhibition through an association with PIR-B

Y Fujita<sup>1,2</sup>, R Takashima<sup>1</sup>, S Endo<sup>3</sup>, T Takai<sup>3</sup> and T Yamashita<sup>\*,1,2</sup>

The Nogo receptor and paired immunoglobulin-like receptor B (PIR-B) are receptors for three myelin-derived axon-growth inhibitors, including myelin-associated glycoprotein (MAG). In this study, we report that the p75 receptor is required for the signal transduction of PIR-B, which interacted with p75 upon ligand binding. In addition, p75 was required for activation of Src homology 2-containing protein tyrosine phosphatase (SHP), which is induced by MAG binding to PIR-B. Mice carrying a mutation in the *p75* gene showed promotion of axonal regeneration after optic nerve injury. Thus, our results indicate that p75 has a critical role in axon growth inhibition in specific neuronal tracts.

*Cell Death and Disease* (2011) 2, e198; doi:10.1038/cddis.2011.85; published online 1 September 2011

**Subject Category:** Neuroscience

Axons in the adult mammalian central nervous system (CNS) have very limited ability to regenerate after injury.<sup>1</sup> Three myelin-associated, structurally distinct proteins—MAG, Nogo, and oligodendrocyte myelin glycoprotein (OMgp)—are considered to be involved in this inhibition of axonal regeneration. These three proteins all bind to the Nogo receptor (NgR) and PIR-B. For signal transduction mediated by NgR, which has no intracellular domain, p75 associates with NgR to transduce the signal inside the cells,<sup>1</sup> acting as a displacement factor that releases RhoA from Rho GDP-dissociation inhibitor.<sup>2</sup> This activation of RhoA has a key role in inducing inhibition of axon growth. In contrast, PIR-B is known to be a receptor for MHC class I and functions as an inhibitory receptor in B cells and myeloid cells.<sup>3</sup> The immunoreceptor tyrosine-based inhibitory motifs (ITIMs) of PIR-B recruit SHP-1 and SHP-2, which, in turn, modulate immune responses. In neurons, PIR-B associates with and inactivates tropomyosin-receptor kinase (Trk) neurotrophin receptors through SHP-1/2.<sup>4</sup> Although this reaction is responsible for axon growth inhibition, the precise mechanism of signal transduction mediated by PIR-B remained to be determined.

p75 is a receptor for neurotrophins and modulates the function of Trk receptors.<sup>5</sup> In some cases, p75 opposes the function of Trk receptors and induces cell death; in other cases, it promotes the function of Trk receptors.<sup>6</sup> These findings prompted us to hypothesize that p75 is involved in the PIR-B-mediated inhibition of Trk receptors.

## Results

**p75 interacts with PIR-B upon ligand binding in neurons.** We first assessed the possible involvement of p75 in the PIR-B signal transduction pathway by performing co-immunoprecipitation experiments in COS-7 cells transfected with plasmids encoding carboxy-terminal hemagglutinin (HA)-tagged full-length p75 (p75 FL-HA) and/or full-length PIR-B (PIR-B FL). Immunoprecipitation was performed using anti-PIR-B or anti-HA antibodies. Of the PIR-B immunoprecipitates, p75 FL-HA was only detected in the p75 FL-HA/PIR-B FL co-transfected cells (Figure 1a). A complementary experiment revealed that PIR-B was also co-immunoprecipitated when an anti-HA antibody was used to immunoprecipitate p75-HA (Figure 1b), providing evidence that p75 associates with PIR-B in transfected COS-7 cells.

Co-immunoprecipitation experiments were then used to identify the molecular determinants of the p75–PIR-B interaction. COS-7 cells were transfected with the PIR-B FL construct, and/or with a construct containing the HA-tagged transmembrane domain and extracellular domain of p75 (p75 ECD + TM-HA). Exogenous p75 ECD + TM-HA was found to co-immunoprecipitate with PIR-B FL when immunoprecipitation was performed with both anti-PIR-B antibodies (Figure 1c) and anti-HA antibodies (Figure 1d). COS-7 cells were then transfected with constructs coding for an HA-tagged p75 intracellular domain (p75-ICD-HA) and/or

<sup>1</sup>Department of Molecular Neuroscience, Graduate School of Medicine, Osaka University, 2-2 Yamadaoka, Suita, Osaka 565-0871, Japan; <sup>2</sup>Japan Science and Technology Agency, Core Research for Evolutional Science and Technology, 5 Sanbancho, Chiyoda-ku, Tokyo 102-0075, Japan and <sup>3</sup>Department of Experimental Immunology and CREST Program of JST, Institute of Development, Aging and Cancer, Tohoku University, Seiryō 4-1, Sendai 980-8575, Japan

\*Corresponding author: T Yamashita, Department of Molecular Neuroscience, Graduate School of Medicine, Osaka University, 2-2 Yamadaoka, Suita, Osaka 565-0871, Japan. Tel: +81 6 68793660; Fax: +81 6 68793669; E-mail: yamashita@molneu.med.osaka-u.ac.jp

**Keywords:** axon regeneration; MAG; p75; PIR-B

**Abbreviations:** PIR-B, paired immunoglobulin-like receptor B; MAG, myelin-associated glycoprotein; SHP, Src homology 2-containing protein tyrosine phosphatase; CNS, central nervous system; OMgp, oligodendrocyte myelin glycoprotein; NgR, Nogo receptor; ITIMs, immunoreceptor tyrosine-based inhibitory motifs; Trk, tropomyosin-receptor kinase; HA, hemagglutinin; FL, full length; ECD, extracellular domain; TM, transmembrane domain; ICD, intracellular domain; P, postnatal day; CGNs, cerebellar granule neurons; WT, wild type; PTP, phosphotyrosine phosphatase; DiFMUP, 6, 8-difluoro-4-methylumbelliferyl phosphate; CTB, cholera toxin beta subunit; KO, knockout; N, N-terminal; C, C-terminal; PFA, paraformaldehyde; DAPI, 4', 6'-diamidino-2-phenylindole; DMEM, Dulbecco's modified Eagle's medium; FBS, fetal bovine serum; PBS, phosphate-buffered solution; SDS-PAGE, sodium dodecyl sulphate-polyacrylamide gel electrophoresis; PVDF, polyvinylidene difluoride; PBS-T, PBS-containing 0.05% Tween-20

Received 22.7.11; accepted 27.7.11; Edited by A Verkhratsky

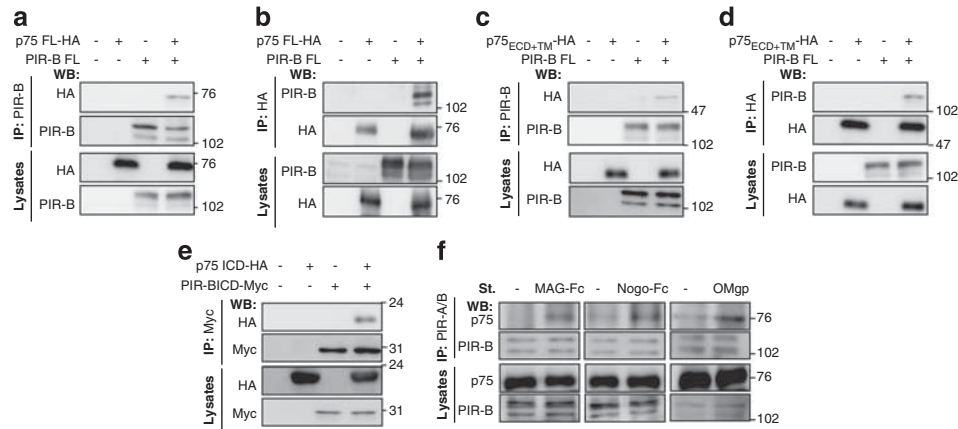


**Figure 1** p75 interacts with PIR-B. (a and b) Co-immunoprecipitation assays to assess the interaction of PIR-B with p75 in COS-7 cells transiently transfected with the indicated plasmids. Lysates were immunoprecipitated with anti-PIR-B (a) or anti-HA (b) antibodies, and western blotting was carried out with the indicated antibodies. Co-immunoprecipitation assays were also used to examine interactions between the following exogenously expressed proteins in transfected COS-7 cells: (c and d) full-length PIR-B with HA-tagged p75 ECD + TM, and (e) HA-tagged p75 ICD with Myc-tagged PIR-B ICD. (f) Co-immunoprecipitation assay demonstrating the interaction of endogenous PIR-B with p75 in unstimulated CGNs or CGNs stimulated with MAG-Fc (25  $\mu$ g/ml), Nogo-Fc (200 nM), or OMgp (2  $\mu$ g/ml) for 30 min. Cell lysates were immunoprecipitated with an anti-PIR-A/B antibody, and western blots were performed with an anti-p75 antibody. (a–f) are representative images from three to four independent experiments. IP, immunoprecipitation

Myc-tagged PIR-B ICD (PIR-B ICD-Myc). The interactions between these ectopically expressed proteins were then examined (Figure 1e), and it was found that the exogenous p75 and PIR-B proteins interact via the intracellular domains, as well as the extracellular domains.

The ligand-dependent interaction of endogenous p75 and PIR-B proteins was also examined in postnatal (day 7) cerebellar granule neurons (CGNs). The CGNs were treated with or without MAG-Fc, Nogo-Fc, or OMgp for 15 min, and the cell lysates immunoprecipitated with PIR-A/B antibody. It was found that the interaction of p75 with PIR-B was enhanced following ligand stimulation (Figure 1f), suggesting that ligand binding to PIR-B promoted the interaction of endogenous PIR-B with p75 in the CGNs.

**p75 associates with PIR-B/TrkB.** As PIR-B associates with Trk receptors to mediate axon growth inhibition,<sup>4</sup> we hypothesized that p75 may also be involved in this signaling complex. The observation that p75 is co-localized with PIR-B and TrkB in immunostained CGNs supports this theory (Figure 2a). In order to further test whether this is the case, we again performed co-immunoprecipitation. To this end, COS-7 cells were co-transfected with constructs for HA-tagged full-length TrkB (TrkB FL-HA), PIR-B FL, and p75 FL-Myc, and the cell lysates were immunoprecipitated with anti-HA, anti-Myc, or anti-PIR-A/B antibodies. Each co-immunoprecipitation experiment detected interactions between TrkB FL-HA, p75 FL-Myc, and PIR-B (Figure 2b). Consistent results were obtained when TrkA was investigated (Figure 2c). The ligand dependency of these interactions was then assessed in CGNs expressing all of these proteins endogenously. The CGNs were treated with or without MAG-Fc or OMgp for 15 min and immunoprecipitated with anti-TrkB, anti-p75, or anti-PIR-B antibodies. TrkB, p75, and PIR-B were again found to interact following both MAG-Fc treatment (Figure 2d, left) and OMgp treatment (Figure 2d, right), supporting the hypothesis that p75

interacts with TrkB and PIR-B upon ligand binding with PIR-B.

We subsequently assessed the requirement of p75 for the association between TrkB and PIR-B by examining the ligand-dependent interaction between TrkB and PIR-B in CGNs in mice carrying a mutation in the *p75* gene.<sup>7</sup> The ligand-dependent interaction was found to be the same in wild-type (WT) mice and in mice carrying a mutation in the *p75* gene (Figure 2e). This is consistent with the results obtained from transfected COS-7 cells (Figure 2b), suggesting that p75 is involved in the PIR-B/Trk receptor complex, but it may not be necessary for the interaction between PIR-B and TrkB.

We also examined whether the kinase activity of TrkB is required for its association with PIR-B. It has previously been reported that Tyr-705/706 of TrkB is phosphorylated upon ligand binding, and that phosphorylation of the Tyr-515 of TrkB is required for interactions with adapter proteins.<sup>5</sup> In our experiments, although PIR-B was co-immunoprecipitated with wild-type TrkB, the level of co-immunoprecipitation with TrkB mutated at Tyr-515 or Tyr-705/706 was significantly reduced (Figure 2f), providing evidence that the kinase activity of TrkB is required for the interaction between TrkB and PIR-B.

**p75 is required for MAG functions in neurons.** We next examined whether p75 is required for the effects mediated by MAG in neurons. Although MAG inhibits neurite growth *in vitro*, this effect is dependent on MAG binding to both NgR and PIR-B. To separate the PIR-B signal from the NgR signal, we focused on the recent finding that MAG stimulation induces dephosphorylation of Trk receptors, which is required for PIR-B-mediated axon growth inhibition.<sup>4</sup> We therefore transfected PIR-B, HA-TrkB, and/or p75-Myc constructs into COS-7 cells, which, as assessed by immunoblot analysis, do not express detectable levels of endogenous PIR-B, TrkB, or p75 (data not shown). These cells were treated with MAG-Fc for 30 min, and the TrkB

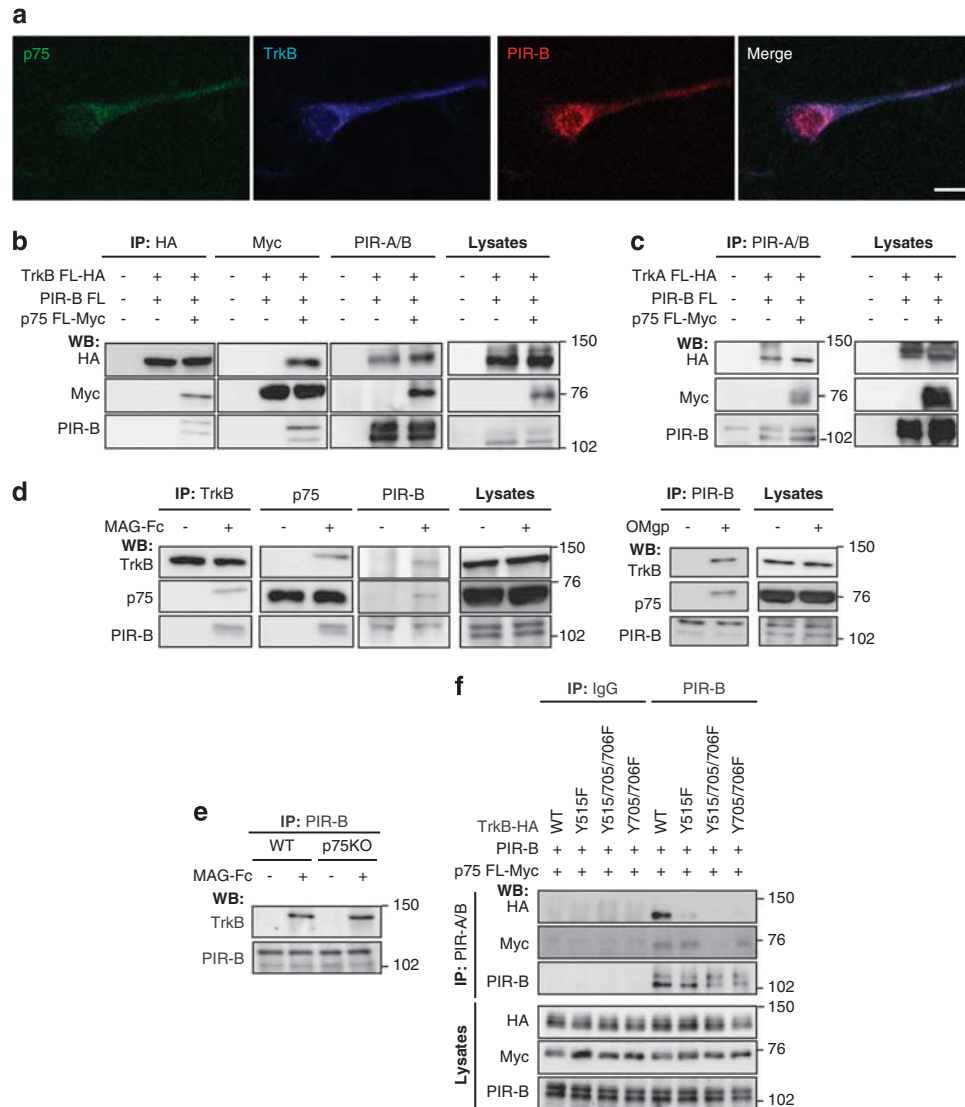


**Figure 2** Interactions between PIR-B, TrkB, and p75 in CGNs. **(a)** CGNs immunostained for p75 (green), PIR-B (red), and TrkB (blue). Scale Bar: 10  $\mu$ m. **(b and c)** Co-immunoprecipitation of the Trk receptors, p75, and PIR-B in COS-7 cells co-expressing combinations of PIR-B FL, and/or p75 FL-Myc with **(b)** TrkB FL-HA or **(c)** TrkA FL-HA. Lysates were immunoprecipitated with the indicated antibodies, followed by western blotting. IP, immunoprecipitation; WB, western blot. **(d)** Co-immunoprecipitation assay of CGNs treated with or without MAG-Fc or OMgp for 15 min. Lysates were immunoprecipitated with the indicated antibodies, and western blotting was carried out. **(e)** Co-immunoprecipitation of TrkB and PIR-B from CGNs obtained from WT and p75-deficient mice (p75 KO). CGNs were treated with or without MAG-Fc for 15 min. **(f)** Co-immunoprecipitation of exogenously expressed TrkB-HA and p75 FL-Myc with PIR-B FL from COS-7 cells. The TrkB-HA expression vectors used were WT TrkB, or TrkB with mutations at Tyr-515 (Tyr-515F), Tyr-705/706 (Tyr-705/706F), or both (Tyr-515/705/706F). Lysates were immunoprecipitated with anti-PIR-A/B antibodies, followed by western blotting with the indicated antibodies

receptors were immunoprecipitated. Their phosphorylation status was then examined using western blotting for phosphotyrosine. It was found that MAG-Fc induced TrkB dephosphorylation in COS-7 cells co-expressing combinations of PIR-B, HA-TrkB, and p75, but not in cells that did not express p75 (Figure 3a). This requirement for p75 in MAG-Fc functions was confirmed using dissociated retinal neurons isolated from mice carrying a mutation in the *p75* gene. These experiments showed that although TrkB is tyrosine dephosphorylated in response to MAG-Fc treatment in WT-dissociated retinal neurons, there was no change in TrkB phosphorylation in the neurons isolated from mice

bearing the *p75* mutation (Figure 3b). Thus, p75 is required for MAG-induced tyrosine dephosphorylation of TrkB receptors. Furthermore, as COS-7 cells co-expressing combinations of PIR-B, HA-TrkB, and the p75 extracellular domain did not exhibit TrkB dephosphorylation upon MAG stimulation, it suggests that the ICD of p75 is required for MAG-induced tyrosine dephosphorylation of TrkB (ECD; Figure 3c).

MAG binding to PIR-B has previously been shown in both CGNs and retinal neurons, to downregulate basal and neurotrophin-regulated Trk activity through the actions of SHP-1/2.<sup>4</sup> We therefore attempted to further delineate the

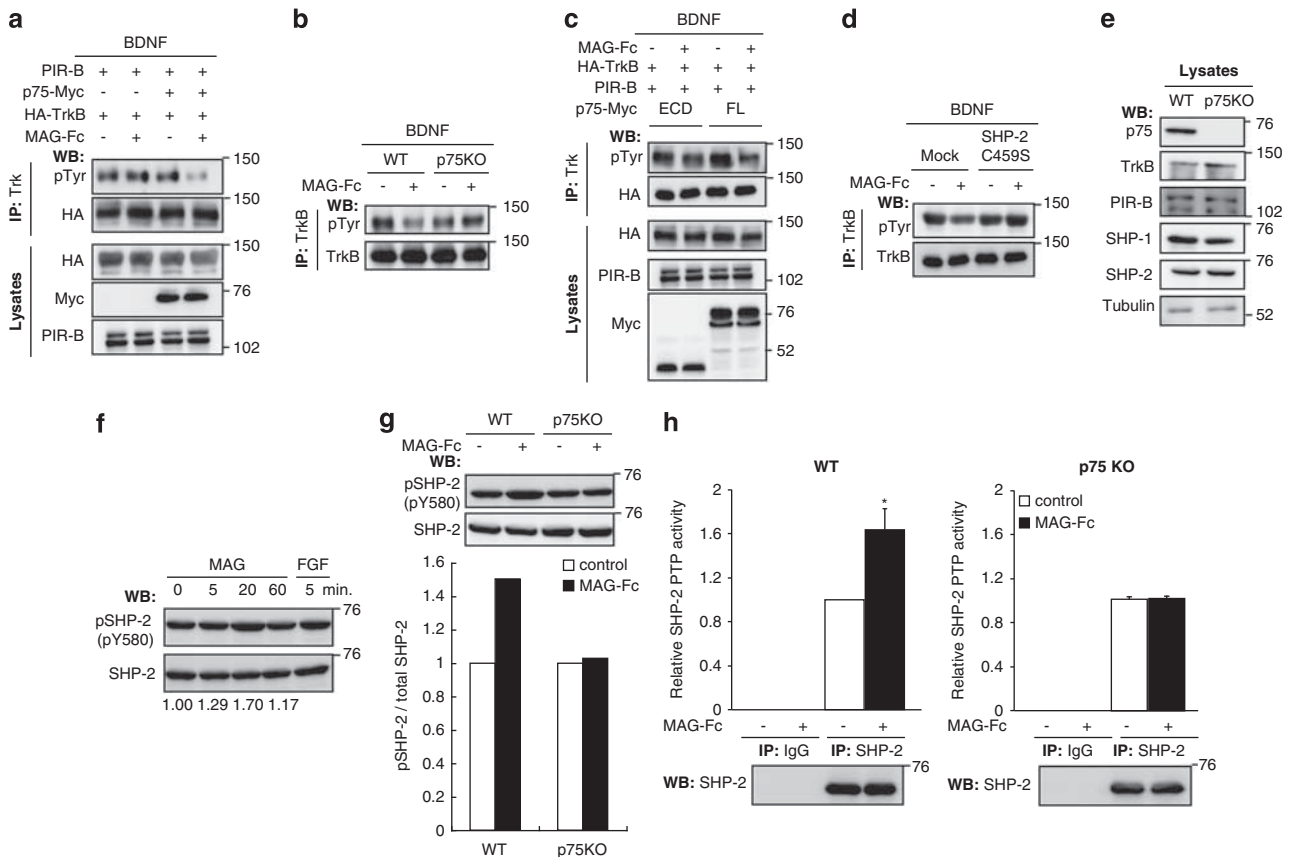


**Figure 3** p75 is required for MAG-induced dephosphorylation of TrkB and SHP activation. (a) Western blots examining the level of TrkB tyrosine phosphorylation in transfected COS-7 cells. The cells were transfected with the indicated constructs and treated with or without MAG-Fc (25  $\mu$ g/ml) for 30 min in the presence of 100 ng/ml BDNF for 5 min. Anti-Trk antibodies were used to immunoprecipitate Trk, and the level of Trk phosphorylation was determined by western blotting with anti-phospho-Tyr antibodies. (b–d) Western blots showing the level of TrkB tyrosine phosphorylation in (b) dissociated retinal neurons from WT and p75 KO mice, (c) transfected COS-7 cells co-expressing TrkB FL-HA and PIR-B FL in combination with p75 FL-Myc or p75 ECD-Myc, and (d) COS-7 cells transfected with or without a construct expressing catalytically inactive SHP-2 (SHP-2 C459S). (e) Western blots showing the expression of the indicated proteins in WT and p75 KO CGNs. (f) Western blots for detecting the levels of phospho-SHP-2 (pTyr-580) and total SHP-2 in CGNs following treatment with MAG-Fc for the indicated periods. FGF (50 ng/ml) was used as a positive control. The relative intensity for the phosphorylated SHP-2 signal is indicated (mean:  $n = 3$ ). (g) Western blots showing phospho-SHP-2 (pTyr-580) and total SHP-2 levels in WT and p75 CGNs. The graph shows relative phospho-SHP-2 levels. (h) Relative SHP-2 PTP activity as measured by PTP assays in CGNs from WT (left) and p75 KO (right) mice. Cells were treated with MAG-Fc for 20 min. \* $P < 0.05$ ; Welch's  $t$ -test

mechanism of TrkB dephosphorylation in response to MAG stimulation. It was found that the transfection of catalytically inactive SHP-2 (SHP-2 C459S) abrogated MAG-induced TrkB dephosphorylation (Figure 3d), suggesting that SHP-2 activity is required for the dephosphorylation of TrkB. Because the expression levels of SHP-1 and SHP-2 were not significantly different between CGNs from WT mice and those from mice carrying a mutation in the *p75* gene (Figure 3e), we hypothesized that SHP activity was enhanced by MAG stimulation. We therefore examined the phosphorylation states of Tyr-542 and Tyr-580 of SHP-2 in CGNs, as the phosphorylation of these sites reflects the catalytic activity of this protein.<sup>8</sup> Immunoblotting with phospho-Tyr-580-specific antibodies revealed that MAG stimulation increased SHP-2 Tyr-580 phosphorylation in a time-dependent manner, with maximal activation at 20 min (Figure 3f). However, there was no change in the SHP-2 phosphorylation level in CGNs from mice carrying a mutation in the *p75* gene (Figure 3g). SHP-2 phosphotyrosine phosphatase (PTP) activity was also determined directly by using fluorogenic 6,8-difluoro-4-methylum-

belliferyl phosphate (DiFMUP) as the substrate in a phosphatase assay, and the relative SHP-2 PTP activity was found to be increased by MAG stimulation in the WT CGNs (Figure 3h, left). In contrast, we observed no enhancement of SHP-2 activity as a result of MAG-Fc treatment in the CGNs from mice bearing the *p75* mutation (Figure 3h, right). These results demonstrate that MAG binding to PIR-B induces SHP-2 activation by a p75-dependent mechanism.

**p75 inhibits axon regeneration *in vivo*.** To assess the relevance of our *in vitro* observations, we also examined the involvement of p75 in axon growth inhibition *in vivo* with the optic nerve crush injury model in 3-week-old mice. Immunohistochemical analysis revealed that although p75 was expressed in the retina before injury (Figure 4a), there was an increase in the level of p75 expression following optic nerve injury (Figure 4b). The regeneration of optic nerve axons was traced by injecting the cholera toxin beta subunit (CTB) conjugated to Alexa Fluor 555 (Invitrogen, Carlsbad, CA, USA) into the vitreous of the retina 12 days after the

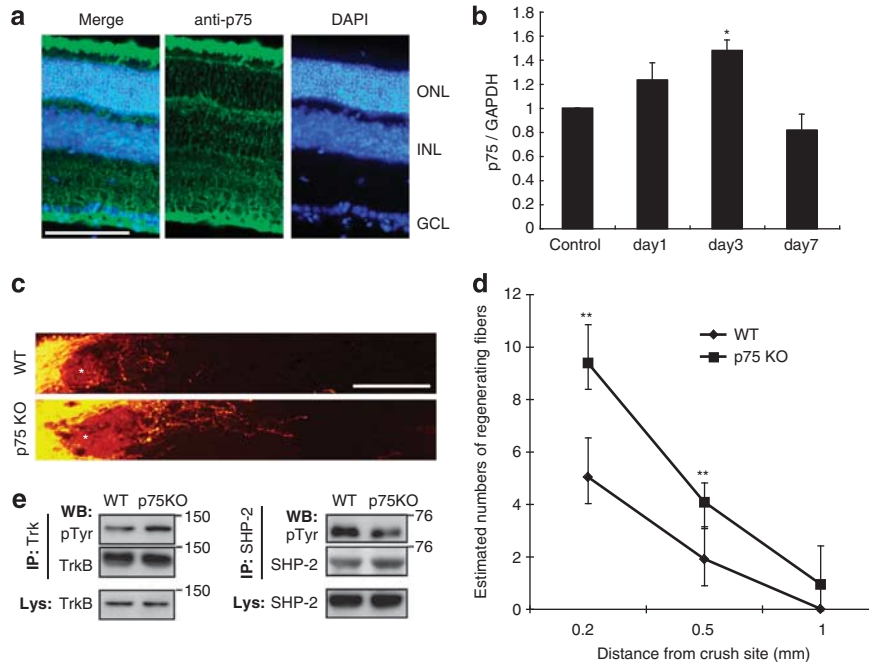


**Figure 4** Axon regeneration following optic nerve injury in p75 KO mice. (a) Immunohistochemical detection of p75 in mouse retinas. The nuclei were stained by 4',6'-diamidino-2-phenylindole (DAPI). Scale bar: 100  $\mu$ m. GCL, ganglion cell layer; INL, inner nuclear layer; ONL, outer nuclear layer. (b) The relative mRNA expression of the p75 gene was examined at the indicated times after optic nerve injury. (c) Longitudinal sections through the optic nerve showing CTB-labeled axons distal to the injury site in WT and p75 KO mice. \*Injury site. Scale bar: 200  $\mu$ m. (d) Quantitative analysis of axon regeneration 14 days after injury. N = 6 (WT), 6 (p75 KO). (e) Western blots showing the phosphorylation levels of TrkB (left) and SHP-2 (right) in extracts from the eye-cups and optic nerves from injured WT or p75 KO mice. \*\* $P < 0.01$ ; two-way ANOVA followed by *post-hoc* Bonferroni analysis

crush injury (Figure 4c). It was found that the optic nerve regeneration 14 days after injury was significantly increased in mice bearing the p75 mutation when compared with WT mice, although the extent of regeneration was not high (Figure 4d). The phosphorylation level of TrkB was also found to be increased (Figure 4e, left), while that of SHP-2 was decreased (Figure 4e, right) in the extracts of the eye-cups and optic nerves prepared from injured p75 knockout (KO) mice. These results indicate that p75 contributes to axon growth inhibition after optic nerve crush injury in mice.

## Discussion

In this study, we show directly for the first time that MAG binding to PIR-B leads to enhancement of SHP activity (Supplementary Figure S1). Intriguingly, p75 is required for this action. SHP-2 belongs to a subfamily of non-transmembrane PTPs that contain 2 N-terminal SH2 domains (N-SH2 and C-SH2), a catalytic domain, and a C-terminal tail with two tyrosyl phosphorylation sites (Tyr-542 and Tyr-580) and a proline-rich motif. In the proposed basal state, SHP-2 is inactive because the 'backside loop' of the N-SH2 domain is associated with catalytic cleft and maintained in a closed state. SHP-2 has been suggested to be activated by C-tail tyrosyl phosphorylation, which may open the enzyme and enable access to the activate site.<sup>8,9</sup> p75 may directly or indirectly regulate these processes. It is also intriguing to hypothesize that SHP regulation by p75 might be a relevant mechanism opposing the function of p75 against Trk

receptors. The precise mechanism of the regulation of SHP activity by p75 will be determined in future studies.

p75 is known to be required for the axon growth inhibition mediated by NgR. Because we found that p75 also participates in PIR-B signal transduction, it appears that p75 is involved in the signals mediated by both the receptors. However, it should be noted that triple-knockout mice lacking all three of the ligands for these receptors show no enhancement in regeneration of the injured corticospinal tract or in motor recovery after spinal cord injury.<sup>10</sup> Results consistent with this were also observed in spinally injured mice that carry a mutation in the p75 gene.<sup>11,12</sup> However, in the optic nerve injury mouse model, we observed regeneration, although not robust, was significant. These seemingly contradictory results might be explained by differences in the p75 expression level in the corresponding tissues. In the optic nerve, p75 is expressed (Figure 4a), whereas p75 expression is weak or undetectable in corticospinal neurons.<sup>11</sup> Therefore, p75 may have a role in inhibiting axon regeneration in specific p75-expressing neurons in the CNS. MAG, Nogo, and OMgp may act as axon growth inhibitors in a neuron-type-specific manner; this issue should be assessed in other neuronal tracts. It should also be noted that SHP inhibition promoted axon regeneration of the injured optic nerves,<sup>4</sup> which is consistent with the findings reported in this study.

We should also consider the finding that p75 transduces the Sema3A signal.<sup>13</sup> Because Sema3A is one of the axon growth inhibitors in the CNS,<sup>14</sup> the *in vivo* data obtained in p75-deficient mice might be the result of a lack of Sema3A signals

independent of the three proteins. In addition, as TrkB activity is upregulated in the retinal neurons from p75NTR KO mice (Figure 4e), the myelin signal is attenuated and TrkB is activated in the p75NTR KO neurons. In conclusion, the present study clearly demonstrates that inhibition of p75 promotes axon regeneration in the CNS and supports the positive role of p75 as an axon growth inhibitory receptor.

### Materials and Methods

**Animals.** We purchased C57BL/6J mice (age, 8 weeks) from Charles River Laboratories. These mice were bred and maintained in the Institute of Experimental Animal Sciences, Osaka University Graduate School of Medicine. We used a C57BL/6J mouse strain bearing a targeted disruption of the third exon of the *p75* gene. The mice were generated by electroporating the targeting vector into the J1 ES cell line derived from a male mouse strain 129 embryo;<sup>7</sup> the strain was originally obtained from Jackson Laboratory (Bar Harbor, ME, USA). All experimental procedures were approved by the Institutional Committee of Osaka University.

**Reagents and antibodies.** The following reagents were used: purified MAG-Fc (25  $\mu$ g/ml), recombinant rat Nogo A-Fc (200 nM; R&D Systems, Minneapolis, MN, USA), mouse OMgp (2  $\mu$ g/ml; R&D Systems), and BDNF (100 ng/ml; Peprotech, Rocky Hill, NJ, USA). Stable CHO cell lines secreting human MAG-Fc were provided by Endo M (Kobe University). The cells were cultured in serum-free medium. Conditioned medium was collected after 3 days, and MAG-Fc was purified with protein A-Sepharose beads. The following antibodies were used: monoclonal anti-HA (HA-7, H3663, 1:5000; Sigma-Aldrich, St Louis, MO, USA), anti-c-Myc, (9E10, sc-40, 1:1000; Santa Cruz Biotechnology, Santa Cruz, CA, USA), anti-SHP-2 (1:1000, BD Transduction Laboratories), biotinylated anti-TrkB (1:2500; R&D systems), anti- $\alpha$ -Tubulin (1:1000; Santa Cruz Biotechnology), and anti-neuronal class III  $\beta$ -tubulin (Tuj1, 1:5000; Covance Laboratories, Inc., Berkeley, CA, USA) antibodies. Polyclonal anti-HA (ab9110, 1:5000; Abcam, Cambridge, UK), anti-p75 (G323A, 1:1000; Promega, Madison, WI, USA), anti-SHP-1, anti-SHP-2, anti-Trk, anti-TrkB, (1:1000; Santa Cruz Biotechnology), anti-PIR-B, (sc-9608 or sc-9609, 1:1000; Santa Cruz Biotechnology), anti-phospho-SHP-2 (1:500; Cell Signaling Technology, Danvers, MA, USA), anti-PIR-B (AF2754, 1 mg/ml; R&D systems), and anti-PIR-A/B (550348, 1:1000; BD Pharmingen, San Diego, CA, USA) antibodies. HRP-linked anti-mouse, anti-rabbit and anti-rat IgG secondary antibodies (Cell Signaling Technology), HRP-linked anti-goat IgG secondary antibody (Santa Cruz Biotechnology), Streptavidin peroxidase (Roche Applied Science, Indianapolis, IN, USA), and Alexa conjugated secondary antibodies (Molecular Probes, Eugene, OR, USA) were used.

**Plasmid constructs and siRNA.** Amino-terminally HA- or Myc-tagged full-length human p75 (NM\_002507) were subcloned into the pcDNA3 vector (Invitrogen, Carlsbad, CA, USA).<sup>15</sup> The extracellular or intracellular domains of p75 were generated from p75-HA. Mouse PIR-B (NC\_000073) was subcloned into the pcDNA3.1Zeo(+) vector as previously described.<sup>16</sup> Rat TrkB (NM\_012731) constructs were provided by Barde Y-A.<sup>17</sup> A mammalian expression vector encoding human TrkA (NM\_001012331, Addgene plasmid 15002)<sup>18</sup> and human SHP-2 C459S (Addgene plasmid 8382) was obtained from Addgene (Cambridge, MA, USA).

Rat TrkB lacking Y515 and/or Y705/706 were made by site-directed mutagenesis.

**Cell culture.** COS-7 cells were cultured in Dulbecco's modified Eagle's medium (DMEM; Invitrogen) containing 10% fetal bovine serum (FBS). Transient transfection of COS-7 cells was performed using Lipofectamine 2000 according to the manufacturer's instructions (Invitrogen). The cells were lysed 24–48 h after the transfection and used for immunoprecipitation. Primary dissociated cultures of CGNs from P7 mice were prepared as reported.<sup>19</sup> After 24 h of plating the neurons on poly-L-lysine-coated dishes, the medium was replaced with DMEM/F12 containing 0.1% BSA. Following 24 h incubation, the neurons were harvested for immunoprecipitation or western blotting. For dissociated retinal cell cultures, P7–P9 mice were used. Eyes were enucleated, and retinas were dissected and incubated at 37°C for 30 min in a digestion solution containing papain (16.5 U/ml; Worthington Biochemical, Lakewood, NJ, USA), DNase (0.5 mg/ml; Sigma-Aldrich), and L-cysteine (0.3 g/ml, Sigma) in phosphate-buffered solution (PBS). Cells were

then rinsed with DMEM containing 10% FBS and centrifuged at 1000 r.p.m for 5 min. To remove cell debris, the cell suspension was passed through a cell strainer (70  $\mu$ m; BD Falcon, Franklin Lakes, NJ, USA). After centrifugation, the supernatant was discarded and the cells were carefully resuspended in DMEM supplemented with B27 (1:50; Invitrogen) or subjected to nucleofection.

**Nucleofection.** Retinal neurons were isolated as described above. The cells were washed and resuspended in room temperature Mouse Neuron Nucleofector Solution (Amaxa; Lonza Cologne AG, Cologne, Germany). The cell–nucleofector solution complex (100  $\mu$ l) and the plasmids (3  $\mu$ g) were then gently mixed and transferred into a cuvette, followed by nucleofection using the nucleofector program O-05 (Lonza, Gaithersburg, MD, USA).

**Co-immunoprecipitation.** Cells were washed with ice-cold PBS and lysed on ice in lysis buffer (50 mM Tris-HCl (pH 7.4), 150 mM NaCl, 0.5–1% NP-40, 10 mM NaF, and 1 mM Na<sub>3</sub>VO<sub>4</sub>) containing protease inhibitor cocktail (Roche Diagnostics, Basel, Switzerland), followed by centrifugation at 4°C with 15000 r.p.m. for 10 min. The supernatants were incubated with the indicated antibodies for 2 h or overnight at 4°C. The immune complexes were collected for 1 h at 4°C with the protein A, protein G-Sepharose (GE Healthcare, Chalfont St. Giles, England), or streptavidin-agarose beads (Thermo Scientific, Waltham, MA, USA) precoated with 0.1–0.5% BSA. After washing the beads thrice with lysis buffer, the proteins were eluted by boiling in 25  $\mu$ l of 2 $\times$  sample buffer for 5 min, and subjected to SDS-PAGE, followed by western blotting. Where indicated, the cells were treated with 25  $\mu$ g/ml MAG-Fc or recombinant human IgG-Fc (R&D systems).

**Western blotting.** Cell lysates were boiled in sample buffer for 5 min. The proteins were separated on sodium dodecyl sulphate-polyacrylamide gel electrophoresis (SDS-PAGE) and transferred onto polyvinylidene difluoride (PVDF) membranes (Millipore, Billerica, MA, USA). The membrane was blocked with 5% non-fat dry milk in PBS containing 0.05% Tween-20 (PBS-T) and incubated for 1 h at room temperature or overnight at 4°C, with the primary antibody diluted in PBS-T containing 1% non-fat dry milk. After washing in PBS-T, the membrane was incubated with horseradish peroxidase-linked anti-mouse IgG antibody, anti-rabbit IgG antibody (Cell Signaling Technology), or Streptavidin-POD (Roche Applied Science). For detection, an ECL chemiluminescence system (GE Healthcare) was used. Signals were detected and quantified using the LAS-3000 image analyzer (Fuji Film, Tokyo, Japan).

**PTP activity assay.** A PTP activity assay was performed as previously described.<sup>20</sup> CGNs were pre-treated with or without MAG-Fc. Cells were lysed in ice-cold PTP lysis buffer (25 mM HEPES, pH 7.4; 150 mM NaCl; 2 mM EDTA; 0.5% Triton X-100) containing a protease inhibitor cocktail. The lysates were incubated with anti-SHP-2 antibody and protein A-Sepharose for 2 h at 4°C. The SHP-2 immune complexes were washed three times with PTP lysis buffer and twice with reaction buffer (20 mM HEPES, pH 7.4; 1 mM EDTA; 5% glycerol; and 1 mM dithiothreitol). The immunoprecipitates were resuspended in 100  $\mu$ l of reaction buffer containing 50  $\mu$ M DiFMUP (Invitrogen) and incubated at room temperature for 20 min. The supernatants were transferred to 96-well plates, and the DiFMUP fluorescence signal was measured at an excitation wavelength of 355 nm and an emission wavelength of 460 nm with a plate reader (Softmax; Molecular Devices, Sunnyvale, CA, USA).

**RNA extraction, reverse transcription, and real-time PCR.** Total RNA was extracted from retinæ by Trizol (Invitrogen) and reverse transcribed using High-Capacity cDNA Reverse Transcription kit (Applied Biosystems, Foster City, CA, USA). The expression of mRNA was examined by real-time PCR using a 7300 Fast Real-Time PCR system (Applied Biosystems). SYBR Green assays were used to quantitate p75. Primers for RGM and neogenin were designed as previously described.<sup>21</sup> The specificity of each primer set was determined with a pre-test showing the specific amplification for a specific gene by gel visualization and sequencing. A sample volume of 20  $\mu$ l was used for SYBR green assays, which contained a 1 $\times$  final concentration of Power SYBR green PCR master mix (Applied Biosystems), 400 nM gene-specific primers, and 1  $\mu$ l template. The PCR cycles started with an UNG digestion stage at 50°C for 2 min, and an initial denaturation period at 95°C lasting for 10 min, followed by 40 cycles at 95°C for 15 s, an annealing phase conducted at 60°C for 1 min, and a gradual increase in temperature from 60 to 95°C during the dissociation stage.

The relative mRNA expression was normalized by measurement of the amount of Gapdh mRNA in each sample. The results of cycle threshold values (Ct values) were calculated by the  $\Delta\Delta C_t$  method to obtain the fold differences.

**Immunohistochemistry.** Cryostat sections were incubated with blocking solution containing 5% BSA and 0.1% Triton X-100 in PBS for 1 h at room temperature, followed by overnight incubation with the primary antibodies at 4°C. Immunoreactivity was visualized using fluorescence-conjugated secondary antibodies. Coverslips were then mounted with mounting medium.

**Optic nerve injury and anterograde labeling.** Optic nerve injury was performed as previously described.<sup>22</sup> Briefly, the left optic nerves of P21 mice were exposed intraorbitally and crushed with fine forceps. On day 12 after axotomy, 2  $\mu$ g of Alexa555-conjugated CTB (Invitrogen) was injected into the vitreous body with a glass needle. On day 14 after axotomy, the animals were perfused with 4% paraformaldehyde (PFA) and the lens and vitreous body were removed. The remaining eye-cup, which contained the nerve segment, was post-fixed and immersed in 10–30% sucrose overnight at 4°C. The eye-cups were then embedded in OCT compound (Tissue Tek; Sakura Finetek, Torrance, CA, USA). Tissues were frozen in dry ice, and 16- $\mu$ m serial cross-sections were prepared using a cryostat and collected on MAS-coated glass slides (Matsunami Glass, Osaka, Japan).

**Quantification of axonal regeneration.** Axonal regeneration was quantified by counting the number of CTB-labeled axons extending 0.2, 0.5, and 1.0 mm from the end of the crush site in four different sections. The cross-sectional width of the nerve was measured at the point where the counts were taken, and used to calculate the number of axons per millimeter of nerve width. This number was then averaged over the five sections. The total number of axons extending the distance  $d$  in a nerve with a radius  $r$  ( $\sum ad$ ) was estimated by summing the number in all the sections with a thickness  $t$  (16  $\mu$ m), using the following formula:

$$\sum ad = \pi r^2 \times (\text{average axons/mm}) / t$$

**Statistical analysis.** The data are presented as the mean  $\pm$  S.E.M. of at least three independent experiments. Statistical analyses were performed using Welch's  $t$ -test (Figure 3h), two-way ANOVA followed by *post-hoc* Bonferroni analysis (Figures 4b and d).  $P$  values of less than 0.05 were considered significant.

#### Conflict of Interest

The authors declare no conflict of interest.

**Acknowledgements.** We thank Ben Neel (Ontario Cancer Institute and Princess Margaret Hospital) and Raymond Birge (New York University School of Medicine) for providing us with the plasmids used in this study.

#### Author contributions

Y.F. and T.Y. conceived the project, and designed the experiments. The project was coordinated and directed by T.Y., with Y.F. performing all experiments. The PTP activity assay and western blots were carried out with the help of R.T., while S.E. constructed the PIR-B expression vector. T.T. provided critical advice for this work, while T.Y. and Y.F. wrote the manuscript.

1. Yiu G, He Z. Glial inhibition of CNS axon regeneration. *Nat Rev Neurosci* 2006; **7**: 617–627.
2. Yamashita T, Tohyama M. The p75 receptor acts as a displacement factor that releases Rho from Rho-GDI. *Nat Neurosci* 2003; **6**: 461–467.
3. Takai T. Paired immunoglobulin-like receptors and their MHC class I recognition. *Immunology* 2005; **115**: 433–440.
4. Fujita Y, Endo S, Takai T, Yamashita T. Myelin suppresses axon regeneration by PIR-B/SHP-mediated inhibition of Trk activity. *EMBO J* 2011; **30**: 1389–1401.
5. Kaplan DR, Miller FD. Neurotrophin signal transduction in the nervous system. *Curr Opin Neurobiol* 2000; **10**: 381–391.
6. Dechant G, Barde YA. The neurotrophin receptor p75(NTR): novel functions and implications for diseases of the nervous system. *Nat Neurosci* 2002; **5**: 1131–1136.
7. Lee KF, Li E, Huber LJ, Landis SC, Sharpe AH, Chao MV *et al*. Targeted mutation of the gene encoding the low affinity NGF receptor p75 leads to deficits in the peripheral sensory nervous system. *Cell* 1992; **69**: 737–749.
8. Lu W, Gong D, Bar-Sagi D, Cole PA. Site-specific incorporation of a phosphotyrosine mimetic reveals a role for tyrosine phosphorylation of SHP-2 in cell signaling. *Mol Cell* 2001; **8**: 759–769.
9. Mohi MG, Neel BG. The role of Shp2 (PTPN11) in cancer. *Curr Opin Genet Dev* 2007; **17**: 23–30.
10. Lee JK, Geoffroy CG, Chan AF, Tolentino KE, Crawford MJ, Leal MA *et al*. Assessing spinal axon regeneration and sprouting in Nogo-, MAG-, and OMgp-deficient mice. *Neuron* 2010; **66**: 663–670.
11. Song XY, Zhong JH, Wang X, Zhou XF. Suppression of p75NTR does not promote regeneration of injured spinal cord in mice. *J Neurosci* 2004; **24**: 542–546.
12. Zheng B, Atwal J, Ho C, Case L, He XL, Garcia KC *et al*. Genetic deletion of the Nogo receptor does not reduce neurite inhibition *in vitro* or promote corticospinal tract regeneration *in vivo*. *Proc Natl Acad Sci USA* 2005; **102**: 1205–1210.
13. Ben-Zvi A, Ben-Gigi L, Klein H, Behar O. Modulation of semaphorin3A activity by p75 neurotrophin receptor influences peripheral axon patterning. *J Neurosci* 2007; **27**: 13000–13011.
14. Togashi H, Schmidt EF, Strittmatter SM. RanBPM contributes to Semaphorin3A signaling through plexin-A receptors. *J Neurosci* 2006; **26**: 4961–4969.
15. Yamashita T, Higuchi H, Tohyama M. The p75 receptor transduces the signal from myelin-associated glycoprotein to Rho. *J Cell Biol* 2002; **157**: 565–570.
16. Endo S, Sakamoto Y, Kobayashi E, Nakamura A, Takai T. Regulation of cytotoxic T lymphocyte triggering by PIR-B on dendritic cells. *Proc Natl Acad Sci USA* 2008; **105**: 14515–14520.
17. Bibel M, Hoppe E, Barde YA. Biochemical and functional interactions between the neurotrophin receptors trk and p75NTR. *Embo J* 1999; **18**: 616–622.
18. Yano H, Lee FS, Kong H, Chuang J, Arevalo J, Perez P *et al*. Association of Trk neurotrophin receptors with components of the cytoplasmic dynein motor. *J Neurosci* 2001; **21**: RC125.
19. Hata K, Kaibuchi K, Inagaki S, Yamashita T. Unc5B associates with LARG to mediate the action of repulsive guidance molecule. *J Cell Biol* 2009; **184**: 737–750.
20. Chen L, Sung SS, Yip ML, Lawrence HR, Ren Y, Guida WC *et al*. Discovery of a novel shp2 protein tyrosine phosphatase inhibitor. *Mol Pharmacol* 2006; **70**: 562–570.
21. Nakamura K, Harada C, Okumura A, Namekata K, Mitamura Y, Yoshida K *et al*. Effect of p75NTR on the regulation of photoreceptor apoptosis in the rd mouse. *Mol Vis* 2005; **11**: 1229–1235.
22. Smith PD, Sun F, Park KK, Cai B, Wang C, Kuwako K *et al*. SOCS3 deletion promotes optic nerve regeneration *in vivo*. *Neuron* 2009; **64**: 617–623.



**Cell Death and Disease** is an open-access journal published by **Nature Publishing Group**. This work is licensed under the **Creative Commons Attribution-NonCommercial-No Derivative Works 3.0 Unported License**. To view a copy of this license, visit <http://creativecommons.org/licenses/by-nc-nd/3.0/>

Supplementary Information accompanies the paper on Cell Death and Disease website (<http://www.nature.com/cddis>)